HDAC and MAPK/ERK Inhibitors Cooperate to Reduce Viability and Stemness Phenotype in Medulloblastoma

Mariane da Cunha Jaeger [1,2] • Eduarda Chiesa Ghisleni [1] • Paula Schoproni Cardoso [1] • Marialva Siniglaglia [1,2] • Tiago Falcon [3] • André T. Brunetto [1,2] • Algemir L. Brunetto [1,2] Caroline Brunetto de Farias [1,2] • Michael D. Taylor [4,5,6,7] • Carolina Nör [4,5] • Vijay Ramaswamy [4,8] • Rafael Roesler [1,9]

[1] Cancer and Neurobiology Laboratory, Experimental Research Center, Clinical Hospital (CPE-HCPA), Federal University of Rio Grande do Sul, Porto Alegre, RS, Brazil

[2] Children's Cancer Institute, Porto Alegre, RS, Brazil

[3] Bioinformatics Core, Experimental Research Center, Clinical Hospital (CPE-HCPA), Porto Alegre, RS, Brazil

[4] The Arthur and Sonia Labatt Brain Tumour Research Centre, The Hospital for Sick Children, Toronto, ON, Canada

[5] Developmental and Stem Cell Biology Program, The Hospital for Sick Children, Toronto, ON, Canada

[6] Department of Laboratory Medicine and Pathobiology, University of Toronto, Toronto, ON, Canada

[7] Division of Neurosurgery, The Hospital for Sick Children, Toronto, ON, Canada

[8] Division of Haematology/Oncology, The Hospital for Sick Children, Toronto, ON, Canada

[9] Department of Pharmacology, Institute for Basic Health Sciences, Federal University of Rio Grande do Sul, Porto Alegre, RS, Brazil

Correspondence: Rafael Roesler

Department of Pharmacology, Institute for Basic Health Sciences, Federal University of Rio Grande do Sul, Rua Sarmento Leite, 500 (ICBS, Campus Centro/UFRGS), 90050-170 Porto Alegre,RS, Brazil.

Telephone: +5551 33083183; fax: +5551 33083121.

E-mail: rafaelroesler@hcpa.edu.br

Abstract

Medulloblastoma (MB), which originates from embryonic neural stem cells (NSCs) or neural precursors in the developing cerebellum, is the most common malignant brain tumor of childhood. Recurrent and metastatic disease is the principal cause of death and may be related to resistance within cancer stem cells (CSCs). Chromatin state is involved in maintaining signaling pathways related to stemness, and inhibition of histone deacetylase enzymes (HDAC) has emerged as a therapeutic tool to target this specific cell population across many tumors. Here, we observed changes in the stemness phenotype induced by HDAC inhibition in MB cells. We treated two human MB cell lines with the HDAC inhibitor (HDACi) sodium butyrate (NaB). Increased acetylation mediated by NaB reduced MB cell viability and expression of stemness markers *BMI1* and *CD133*. In addition, activation of extracellular-regulated kinase (ERK) signaling was also decreased after treatment with NaB. We went on to use the mitogen-activated protein kinase kinase (MEK) inhibitor U0126 to explore the role of the mitogen-activated protein kinase (MAPK)/ERK pathway in the stemness phenotype. MEK inhibition reduced the expression of the stemness markers and, when combined with NaB, the antiproliferative effect was enhanced. Inhibition of MAPK/ERK activity hindered MB neurosphere formation, supporting the possibility that this pathway is involved in regulating stemness in MB. These results suggest that combining HDAC and MAPK/ERK inhibitors may be more effective in reducing MB proliferation than single-drug treatments, through modulation of the stemness phenotype of MB cells.

Keywords Medulloblastoma ● Histone deacetylase ● BMI1 ● Stemness ● Cancer stem cell ● Brain tumor

Introduction

Medulloblastoma (MB), the most common malignant pediatric brain tumor, likely arises from genetic and epigenetics abnormalies during cerebellar development [1]. Integrative genomic, epigenomic and transcriptional analyses have shown that MB is not a single tumor type. Instead, it is comprised of at least four molecular subgroups: Wingless (WNT), Sonic hedgehog (SHH), Group 3 and Group 4, that also have distinct demographic, clinical, and prognostic features [2]. The WHO 2016 classification of central nervous system (CNS) tumors divides MB in WNT-MB, SHH-MB/*TP53* wild type, SHH-MB/*TP53* mutated, Group 3 and Group 4 [3]. This molecular identification of MB subgroups has resulted in several clinical trials of subgroup specific therapies, however, except for de-escalation of therapy for WNT patients, there are a paucity of new treatment options for most patients. Specifically, the long-term neurocognitive sequelae of therapy affect the life quality of MB survivors while patients with recurrent and metastatic disease usually succumb to their disease [4, 5].

According to the cancer stem cell (CSC) hypothesis, recurrence and metastasis in some tumor types may arise from a specific tumor cell subpopulation, the CSC, a distinct population of cells presenting stem cell-like properties such as clonal long-term repopulation and self-renewal capacity [6, 7]. In some cancers, including CNS tumors, CSCs drive tumor initiation and progression and are able to recapitulate the phenotype of the tumor from which they were derived [8]. In MB, CSCs are identified by the expression of neural stem cell (NSC) markers such as *CD133*, *BMI1*, *Nestin* and *Sox2*, by their capacity to form neurospheres *in vitro*, and by

tumorigenicity in animal xenograft models [8, 9]. These highly tumorigenic cells display features including stemness, therapeutic resistance, and invasion [10-14].

Given that a failure in maturation of cerebellar progenitor cells is likely at the origin of MB, and the resistance characteristics presented by CSCs may be responsible for therapeutic failure, modulation of cellular differentiation may be seen as a relevant strategy. In this context, epigenetic modulators have emerged as an exciting therapeutic avenue, particularly histone deacetylase inhibitors (HDACis) [15, 16]. HDACs are enzymes that control, in a balance with histone acetyltransferases (HATs), histone acetylation regulating chromatin state. HDACis promote the acetylation of histones and non-histone proteins, modify gene expression profiles, and regulate many biological processes involved in tumor homeostasis, such as apoptosis, cell-cycle arrest, angiogenesis, and differentiation [16]. HDACi play a role as differentiation inducers in several childhood cancers including neuroblastoma [17], Ewing sarcoma [18] and MB [19]. In MB, the antiproliferative effect of HDACi is accompanied by morphological changes, cell cycle arrest, increased expression of glial and neuronal markers, and reduced tumorigenicity [20-25]. We have previously shown that sodium butyrate (NaB), a class I and IIa HDACi, decreases neurosphere formation in MB cultures [23]. Using different HDACis, a recent study found a similar effect on neurosphere survival, even in the absence of significant changes in the expression of the stemness marker *CD133* [24].

Given that the stemness phenotype is proposed as a poor prognostic marker in many cancer types including MB [26, 27] and the effects of HDACi in regulating stemness are still not fully understood, the aim of this study was to investigate how NaB influences aspects of the stemness phenotype of MB cells. We examined the expression of *BMI-1*, a potent inducer of NSC self-renewal and neural progenitor proliferation during cerebellar development [28], and activation of

extracellular-regulated kinase (ERK), which plays a role in maintenance of pluripotency in normal human stem cells [29], in MB cells after treatment with NaB.

Materials and Methods

Cell Culture

Human Daoy (HTB186™) and D283 Med (HTB185™) MB cells were obtained from the American Type Culture Collection (ATCC, Rockville, USA). Cells were maintained in tissue culture flasks at 37 °C with humidified atmosphere and 5 % CO_2. The culture medium, which was changed every 2/3 days, was prepared with DMEM (Gibco, Grand Island, USA), 1% penicillin and streptomycin (Gibco), supplemented with 10 % fetal bovine serum (Gibco), with the pH adjusted to 7.4.

Treatments and Cell Viability

MB cells were seeded at 18.000 cells/well in 24 wells plates. After 24 h, cells were treated with the HDAC inhibitor NaB (Sigma-Aldrich, St. Louis, USA) alone or in combination with the MEK1/2 inhibitor U0126 (12.5 or 25 µM, Sigma-Aldrich). The NaB doses used in Daoy (0.25, 1.0, or 2.5 mM) and D283 (0.5, 2.5, or 5.0 mM) cells were chosen in agreement with a protocol

previously described [23]. Forty-eight hours after treatment, cells were trypsinized and counted in a Neubauer chamber with trypan blue (10 µl dye to each 10 µl cell suspension) for viability measurement.

Histone H3 Acetylation

Cells treated for 48 h with NaB were lysed with a lysis solution buffer and acetylation of H3 was measured with PathScan® Acetylated Histone H3 Sandwich enzyme-linked immunosorbent assay (ELISA) Kit (Cell Signaling Technology, Danvers, USA) according to the manufacturer's instructions. Colorimetric signals were measured by spectrophotometric determination (OD450 nm) on Biochrom® Anthos Zenyth 200 Microplate Reader.

Gene Expression Correlation and Enrichment Analysis

We analyzed data from 763 MB samples [30] to detect genes significantly correlated ($p < 0.05$) with both *CD133* or *BMI1* expression and to perform enrichment analysis of the correlated genes using the R2: Genomics Analysis and Visualization Platform (http://r2.amc.nl). KEGG results and Gene Ontology Biological Process pathways were checked again and plotted using the R software environment v.3.4.4 [31] and the R package pathfindR v.1.2.1 [32] considering as significantly enriched pathways those with FDR < 0.05 in the function *run_pathfindR*. This function requires as input a dataset containing the gene identification (we used the HUGO symbol) the log fold

change and corrected p-value of their expression to perform the cut-off. Here, we replaced the fold change for the r (correlation) value and the p-value for the p-value of this correlation. Thus, we could indicate those negatively and positively correlated genes with either *BMI1* or *CD133*.

Reverse Transcriptase Polymerase Chain Reaction (RT-qPCR)

The mRNA expression of stemness markers was analysed by RT-qPCR. Total RNA was extracted from MB cells using SV Total RNA Isolation System kit (Promega, Madison, USA), in accordance with the manufacturer's instructions and quantified in NanoDrop (Thermo Fisher Scientific, Waltham, USA). The cDNA was obtained using GoScript Reverse System (Promega) according to the manufacturer's instructions. The mRNA expression levels of target genes (*BMI1* and *CD133*) were quantified using PowerUp SYBR Green Master Mix (Thermo Fisher Scientific.) The primers used for RT-qPCR amplification were designed according to the corresponding GenBank and are shown in Table 1. Expression of β-actin was measured as an internal control.

Western Blot

Cells were lysed after NaB treatment with 1X Lysis Buffer (Cell Lysis Buffer 10X, Cell Signaling Technology), and protein was quantified using the Bradford protein assay (Thermo Scientific). For blotting, 20 µg of protein were separated by SDS-PAGE and transferred to a PVDF membrane. After 1h with blocking solution (5%BSA in TTBS), the membrane was incubated overnight at 4

°C with primary antibodies against BMI1 (1:1000; Cell Signaling), Phospho-p44/42 MAPK (pErk1/2, 1:2000; Cell Signaling), p44/42 MAPK (Erk1/2, 1:1000; Cell Signaling) and β-actin (1:2000; Santa Cruz Biotechnology) as protein control. Incubation of primary antibodies was followed by incubation with the secondary antibody (1:2000; Sigma Aldrich) for 2 h. Chemoluminescence was detected using ECL Western Blotting substrate (Pierce, Thermo Scientific) and analyzed using ImageQuant LAS 500 (GE Healthcare Life Sciences, Little Chalfont, UK). Immunodetection signal were analyzed using ImageJ (National Institutes of Health, Bethesda, USA).

Neurosphere Formation

Neurosphere formation was used as an established experimental assay to evaluate cancer stem cell proliferation [23,33]. Daoy and D283 cells were dissociated with trypsin-EDTA into a single cell suspension and seeded at 500 cells/well in 24-well low-attachment plates. The cells were cultured in serum-free sphere-induction medium, containing DMEM/F12 supplemented with 20 ng/ml epidermal growth factor (EGF, Sigma-Aldrich), 20 ng/ml basic fibroblast growth factor (Sigma-Aldrich), B-27 supplement 1X (Gibco), N-2 supplement 0.5X (Gibco), 50 μg/ml bovine serum albumin (Sigma Aldrich), and antibiotics during 7 days as previously described [23]. The ERK inhibitor U0126 was added in the first day after plating cells with the sphere-induction medium. Spheres photomicrographs were captured 7 days after treatment under an inverted phase microscope (Leica Microsystems, Mannheim Germany) at×10 magnification.

Statistics

Data are shown as mean ± standard deviation (SD). Statistical analysis was performed by one-way analysis of variance (ANOVA) followed by Tukey post-hoc tests for multiple comparisons. Experiments were replicated at least three times; *P* values under 0.05 were considered to indicate statistical significance. The GraphPad Prism 6 software (GraphPad Software, San Diego, USA) was used for analyses.

Table 1 should be inserted here

Results

HDAC Inhibition Impairs MB Cell Viability

Direct cell quantification after 48-h treatment with escalating doses of NaB confirmed a significant reduction in cell viability of both Daoy and D283 relative to vehicle. Consistently with a previous report [23], Daoy cells presented a somewhat higher sensibility to NaB than D283 cells. A dose of 2.5 mM reduced viability to 41.7% of control levels in Daoy cells ($P<0.0001$), whereas the same dose decreased D283 cell viability to 71% of control levels ($P<0.0001$). Lower doses of NaB,

namely 0.25 mM in Daoy and 0.5 mM in D283 cells, did not significantly change cell numbers **(Fig. 1a)**.

In order to evaluate a biochemical indicator of efficacy, histone H3 acetylation was measured by ELISA in cells treated for 48 h. The effective doses of NaB (1.0 and 2.5 mM in Daoy, and 2.5 and 5.0 mM in D283) induced 2.42-fold and 3.03-fold increases (Daoy, $P < 0.0001$) and 2.5-fold and 5.7-fold increases (D283, $P = 0.005$ and $P < 0.0001$, respectively) in the levels of acetylated H3 compare to controls **(Fig. 1b)**. Notably, the levels of acetylated H3 were inversely correlated to the effect on cell viability.

Fig. 1 should be inserted here

HDAC Inhibition Reduces the Expression of Stemness Markers and ERK Activation in MB Cells

To elucidate whether NaB could suppress MB viability by modulating the stemness phenotype, expression of *BMI1* and *CD133* was analyzed after 48 h of NaB treatment. The both marks are expressed in all molecular subgroups of MB as observed in Cavalli et al. (2017) samples **(Fig. 2a)**. Experiments using RT-qPCR showed a reduction in mRNA levels of stemness markers *BMI1* and *CD133***.** In Daoy cells, mRNA expression of *BMI1* was reduced in cells treated with the higher dose of NaB (2.5 mM; $P = 0.0007$), whereas all doses of NaB (0.25, 1.0, and 2.5 mM) reduced *CD133* expression compared to controls (0.25 mM, $P = 0.018$; 1 mM, $P = 0.01$; 2.5 mM, $P =$

0.0006). In D283 cells, both doses that were effective when used in cell counting experiments (2.5 and 5 mM) reduced *BMI1* expression (2.5 mM, p = 0.0017; 5 mM, $P < 0.0001$), and *CD133* expression was reduced by all doses (0.5 mM, $P = 0.0198$; 2.5 mM and 5 mM, $P < 0.0001$) **(Fig. 2b)**.

The reduction in protein levels of BMI1 was confirmed after 24 h of NaB treatment in both cell lines at any dose capable of significantly impairing cell viability. After a 48-h treatment, Daoy cells maintained a consistent reduction in BMI1 protein levels compared to controls, and a significant reduction was found in D283 cells treated with the highest dose (5 mM) compared to controls ($P = 0.0023$) **(Fig. 2c)**.

Fig. 2 should be inserted here

MAPK/ERK signaling regulates normal CNS development. The enrichment analysis of the genes significantly correlated with *CD133* or *BMI1* expression showed MAPK signaling or associated pathways (like Neurotrophin and Erb signaling) as the most enriched process **(Fig. 3a, Supplementary Table S1, S2, Supplementary Fig. S1, S2)**. To investigate the status of the MAPK/ERK pathway in the MB cells after treatment with NaB, Western blotting was performed. NaB at any dose led to a decrease in ERK pathway activation measured by ERK phosphorylation in both cell lines after 48 h. Even in non-effective doses (0.25 mM in Daoy and 0.5 mM in D283 cells), a reduction of about 20% was observed, whereas doses that significantly affect cell viability reduced ERK activation in both cell lines *P*s < 0.0001) **(Fig. 3b, c)**.

Fig. 3 should be inserted here

HDAC and MAPK/ERK Inhibition Cooperate to Reduce MB Growth

To determine the effect of ERK inhibition on stemness markers in MB cells, mRNA expression of *BMI1* and *CD133* was measured after 48 h of treatment with the MEK1/2 inhibitor U0126 (12.5, or 25 μM). *CD133* expression decreased significantly after treatment in both cell lines (Daoy, $P = 0.0001$ and $P < 0.0001$; D283, $P = 0.02$ and $P < 0.0001$). Reductions in *BMI1* were observed in both cell lines (Daoy, 12.5 μM, $P = 0.0094$; 25 μM, $P = 0.0016$; D283, 25 μM, $P = 0.0436$) **(Fig. 4a)**.

Given that there is a possible relationship between the stemness phenotype and cell viability, cell counting after treatment with U0126 with or without NaB was performed. U0126 (25 μM) significantly reduced MB cell viability (Daoy, $P = 0.0008$; D283, $P < 0.0001$). Combined treatment of the highest dose of U0126 (25 μM) plus NaB (1.0 or 2.5 mM in Daoy and 2.5 or 5

mM in D283) produced more robust inhibition of cell proliferation than either inhibitor alone at the same doses in both cell lines. **(Fig. 4b)**.

Fig. 4 should be inserted here

MAPK/ERK Inhibition Hinders the Expansion of Putative MB CSCs

A neurosphere assay was performed to investigate the formation of MB CSCs. First, the mRNA expression of *CD133* and *BMI1* was measured to confirm enrichment of stemness after sphere formation. Expression of both markers was increased in neurospheres compared to monolayer cultures. After 7 days of culturing cells in appropriated medium for expansion of stem cells, *BMI1* expression was increased 1.68-fold in Daoy ($P = 0.0006$) and to 2.0-fold in D283 ($P = 0.0028$) cells, while *CD133* expression increased 2.89-fold in Daoy ($P = 0.0005$) and to 2.36-fold in D283 ($P < 0.0001$) cells in comparison to controls **(Fig. 5a)**. After MAPK/ERK inhibition (12.5 or 25 μM), cells were unable to form neurospheres **(Fig. 5b)**. These results suggest an essential role of ERK signalling in MB stem cell formation.

Fig. 5 should be inserted here

Discussion

MB is a pediatric brain tumor featuring a high frequency of mutations in epigenetic modifier genes [34,35]. Deregulation in epigenetic programming has been linked to tumorigenesis, possibly through induction of a stemness phenotype [36]. Histone acetylation status is related to cancer stemness regulation, and HDAC inhibition constitutes an important therapeutic strategy to induce differentiation in CSCs [37].

We have previously shown responsiveness of human MB cells and putative MB CSCs to NaB [23]. Here, we used the same compound to investigate the influence of HDAC inhibition on maintenance of a stemness phenotype of MB. We confirmed that the effect of NaB is associated with its capability to increase histone acetylation. We have also shown a reduction in markers of stemness and inhibition of MAPK/ERK signalling. Moreover, HDAC and MEK1/2 inhibitors cooperate to reduce viability in MB cells and, as with HDACi, MAPK/ERK inhibition hinders neurosphere formation.

Expression of *CD133* and *BMI1* was significantly decreased after NaB treatment. CD133, also called Prominin-1, is the most used marker to isolate and to identify brain tumor CSCs [38]. BMI1 is a polycomb group protein overexpressed in MB [28] and present in CSC [39]. Patients with metastatic MB show higher levels of *CD133* and a worse prognostic when compared with non-metastatic patients [40]. *In vitro* characterization of CD133-positive cells demonstrates that they present increased migration and invasion capabilities and higher expression of stemness-associated genes compared to the parental cell line. In addition, CD133-positive, but not CD133-negative cells, are invasive *in vivo* [41, 42]. These functional features of CD133-positive cells are

associated with a stemness genetic signature. The volume of xenografted tumors is reduced by treatments that inhibit the expression of stemness-related genes such as *SOX2*, *Nestin*, *Nanog*, *Oct4* and *BMI1* [42, 43]. BMI-1, another marker of poor outcomes in MB [43], is also involved in tumor invasion, as indicated by evidence that BMI1 knockdown in MB cells decreases infiltration of xenotransplants [44].

We observed a decrease in phosphorylated ERK (pERK) in MB cells after NaB treatment. Components of the ERK pathway are up-regulated in metastatic MB, and pharmacological inhibition of ERK decreases migration of MB cells [45]. In carcinoma and sarcoma cell lines, ERK reduces the stem-like characteristics of tumor cells [46]. In our study, ERK inhibition reduced the expression level of stemness markers and enhanced the antiproliferative effect of NaB. In agreement with our results, Ozaki and colleagues have shown an increase in HDACi-induced cell death after specific inhibition of the ERK pathway by the generation of reactive oxygen species [47, 48]. Although our study has not evaluated the mechanisms mediating functional interactions between HDAC and ERK inhibitors, our findings suggest that both types of compounds are involved in stemness modulation.

The influence of ERK activity in regulating the stemness phenotype was showed in a neurosphere model [49]. Expansion of neurospheres resulted in an enrichment of the stemness phenotype in cell cultures, as indicated by increased levels of *CD133* and *BMI1* content in comparison with a monolayer culture. We found that pharmacological inhibition of ERK impairs MB neurosphere formation. The role of ERK signaling was already described in other tumor stem-like cells [50,51]. In embryonal rhabdomyosarcoma stem-like cells, the inhibition of ERK decrease sphere formation, induce myogenic differentiation, and reduce tumorigenicity *in vivo* [50]. In glioblastoma CSCs, ERK inhibition also limited the capacity to form tumors in nude mice and

promote cell differentiation. Consistently with our results, ERK inhibition of glioblastoma CSCs reduces the expression of stemness markers, including *BMI1* [51].

In MB, Chow and collegues showed differential ERK signalling activation and neurosphere formation capability in MB cells from spontaneous tumors obtained from Patched (Ptch)+/- mice [52]. Tumors that were able to form neurospheres independently of the presence of growth factors (EGF and basic fibroblast growth factor) had a higher activation of the ERK pathway compared to those tumors dependent on growth factors or not capable of forming spheres. Interestingly, tumors derived from growth factors independent neurospheres cells presented higher tumorigenicity potential and lethality [52].

In summary, our results provide evidence indicating that HDAC inhibition can modulate the stemness phenotype, by reducing the expression of stemness markers *CD133* and *BMI1*, and decreasing ERK activity, in MB. Combined inhibition of HDAC and ERK signaling was more effective in reducing MB cell viability than single-drug treatments. To our knowledge, this is the first report to indicate that ERK inhibition impairs MB CSC formation/survival. We suggest the combination of HDAC and ERK inhibitors as an experimental therapeutic approach in MB, which should be further investigated with the use of additional experimental approaches such as *in vivo* models.

Acknowledgements

This research was supported by the National Council for Scientific and Technological Development (CNPq; grant numbers 303276/2013-4 and 409287/2016-4 to R.R., grant number 201001/2014-4 to C.N., and graduate fellowship to M.C.J.); PRONON/Ministry of Health, Brazil (number 25000.162.034/2014-21); the Children's Cancer Institute (ICI); the Rio Grande do Sul State Research Foundation (FAPERGS; grant number 17/2551-0001 071-0 to R.R.); the Coordination for the Improvement of Higher Education Personnel; and the Clinical Hospital institutional research fund (FIPE/HCPA). T.F. is supported by Programa Nacional de Pós-Doutorado (PNPD, CAPES/HCPA, grant number: 88887.160608/2017-00). C.N. is also supported by the William Donald Nash fellowship from the Brain Tumour Foundation of Canada. V.R. is supported by operating funds from the Canadian Institutes for Health Research, the American Brain Tumour Association, and the Brain Tumour Foundation of Canada. M.D.T. is supported by the National Institutes of Health, The Pediatric Brain Tumour Foundation, The Terry Fox Research Institute, The Canadian Institutes of Health Research, The Cure Search Foundation, b.r.a.i.n.child, Meagan's Walk, Genome Canada, Genome BC, the Ontario Institute for Cancer Research, and the Canadian Cancer Society Research Institute.

References

1. Wang J, Wechsler-Reya RJ (2014) The role of stem cells and progenitors in the genesis of medulloblastoma. Exp Neurol 260: 69-73.

2. Taylor MD, Northcott PA, Korshunov A, Remke M, Cho YJ, Clifford SC, Eberhart CG, Parsons DW, et al. (2012) Molecular subgroups of medulloblastoma: the current consensus. Acta Neuropathol 123: 465-472.

3. Louis DN, Perry A, Reifenberger G, von Deimling A, Figarella-Branger D, Cavenee WK, Ohgaki H, Wiestler OD, et al. (2016) The 2016 World Health Organization Classification of Tumors of the Central Nervous System: a summary. Acta Neuropathol 131: 803-820.

4. Schwalbe EC, Lindsey JC, Nakjang S, Crosier S, Smith AJ, Hicks D, Rafiee G, Hill RM, et al. (2017) Novel molecular subgroups for clinical classification and outcome prediction in childhood medulloblastoma: a cohort study. Lancet Oncol 18: 958-971.

5. Sabel M, Fleischhack G, Tippelt S, Gustafsson G, Doz F, Kortmann R, Massimino M, Navajas A, et al. (2016) Relapse patterns and outcome after relapse in standard risk medulloblastoma: a report from the HIT-SIOP-PNET4 study. J Neurooncol 129: 515-524.

6. Peitzsch C, Tyutyunnykova A, Pantel K, Dubrovska A (2017) Cancer stem cells: The root of tumor recurrence and metastases. Semin Cancer Biol 44: 10-24.

7. Kreso A, Dick JE (2014) Evolution of the cancer stem cell model. Cell Stem Cell 14: 275-291.

8. Singh SK, Hawkins C, Clarke ID, Squire JA, Bayani J, Hide T, Henkelman RM, Cusimano MD, et al. (2004) Identification of human brain tumour initiating cells. Nature 432: 396-401.

9. Hemmati HD, Nakano I, Lazareff JA, Masterman-Smith M, Geschwind DH, Bronner-Fraser M, Kornblum HI (2003) Cancerous stem cells can arise from pediatric brain tumors. Proc Natl Acad Sci U S A 100: 15178-15183.

10. Hambardzumyan D, Becher OJ, Rosenblum MK, Pandolfi PP, Manova-Todorova K, Holland EC (2008) PI3K pathway regulates survival of cancer stem cells residing in the perivascular niche following radiation in medulloblastoma in vivo. Genes Dev 22: 436-448.

11. Annabi B, Rojas-Sutterlin S, Laflamme C, Lachambre MP, Rolland Y, Sartelet H, Beliveau R (2008) Tumor environment dictates medulloblastoma cancer stem cell expression and invasive phenotype. Mol Cancer Res 6: 907-916.

12. Lu KH, Chen YW, Tsai PH, Tsai ML, Lee YY, Chiang CY, Kao, CL, Chiou SH, et al. (2009) Evaluation of radiotherapy effect in resveratrol-treated medulloblastoma cancer stem-like cells. Childs Nerv Syst 25: 543-550.

13. Yu CC, Chiou GY, Lee YY, Chang YL, Huang PI, Cheng YW, Tai LK, Ku HH, et al. (2010) Medulloblastoma-derived tumor stem-like cells acquired resistance to TRAIL-induced apoptosis and radiosensitivity. Childs Nerv Syst 26: 897-904.

14. Liu J, Chi N, Zhang JY, Zhu W, Bian YS, Chen HG (2015) Isolation and characterization of cancer stem cells from medulloblastoma. Genet Mol Res 14: 3355-3361.

15. Klonou A, Spiliotakopoulou D, Themistocleous MS, Piperi C, Papavassiliou AG (2018) Chromatin remodeling defects in pediatric brain tumors. Ann Transl Med 6: 248.

16. Ververis K, Hiong A, Karagiannis TC, Licciardi PV (2013) Histone deacetylase inhibitors (HDACIs): multitargeted anticancer agents. Biologics 7: 47-60.

17. Frumm SM, Fan ZP, Ross KN, Duvall JR, Gupta S, VerPlank L, Suh BC, Holson E, et al. (2013) Selective HDAC1/HDAC2 inhibitors induce neuroblastoma differentiation. Chem Biol 20: 713-725.

18. Souza BK, da Costa Lopez PL, Menegotto PR, Vieira IA, Kersting N, Abujamra AL, Brunetto AT, Brunetto AL, et al. (2018) Targeting histone deacetylase activity to arrest cell growth and promote neural differentiation in Ewing sarcoma. Mol Neurobiol 55: 7242-7258.

19. Li XN, Parikh S, Shu Q, Jung HL, Chow CW, Perlaky L, Leung HC, Su J, et al. (2004) Phenylbutyrate and phenylacetate induce differentiation and inhibit proliferation of human medulloblastoma cells. Clin Cancer Res 10: 1150-1159.

20. Sonnemann J, Kumar KS, Heesch S, Muller C, Hartwig C, Maass M, Bader P, Beck JF (2006) Histone deacetylase inhibitors induce cell death and enhance the susceptibility to ionizing radiation, etoposide, and TRAIL in medulloblastoma cells. Int J Oncol 28: 755-766.

21. Spiller SE, Ditzler SH, Pullar BJ, Olson JM (2008) Response of preclinical medulloblastoma models to combination therapy with 13-cis retinoic acid and suberoylanilide hydroxamic acid (SAHA). J Neurooncol 87: 133-141.

22. Marino AM, Sofiadis A, Baryawno N, Johnsen JI, Larsson C, Vukojevic V, Ekstrom TJ (2011) Enhanced effects by 4-phenylbutyrate in combination with RTK inhibitors on proliferation in brain tumor cell models. Biochem Biophys Res Commun 411: 208-212.

23. Nor C, Sassi FA, de Farias CB, Schwartsmann G, Abujamra AL, Lenz G, Brunetto AL, Roesler R (2013) The histone deacetylase inhibitor sodium butyrate promotes cell death and differentiation and reduces neurosphere formation in human medulloblastoma cells. Mol Neurobiol 48: 533-543.

24. Yuan J, Llamas Luceno N, Sander B, Golas MM (2017) Synergistic anti-cancer effects of epigenetic drugs on medulloblastoma cells. Cell Oncol (Dordr) 40: 263-279.

25. Phi JH, Choi SA, Kwak PA, Lee JY, Wang KC, Hwang DW, Kim SK (2017) Panobinostat, a histone deacetylase inhibitor, suppresses leptomeningeal seeding in a medulloblastoma animal model. Oncotarget 8: 56747-56757.

26. Glinsky GV, Berezovska O, Glinskii AB (2005) Microarray analysis identifies a death-from-cancer signature predicting therapy failure in patients with multiple types of cancer. J Clin Invest 115: 1503-1521.

27. Shats I, Gatza ML, Chang JT, Mori S, Wang J, Rich J, Nevins JR (2011) Using a stem cell-based signature to guide therapeutic selection in cancer. Cancer Res 71: 1772-1780.

28. Leung C, Lingbeek M, Shakhova O, Liu J, Tanger E, Saremaslani P, Van Lohuizen M, Marino S (2004) Bmi1 is essential for cerebellar development and is overexpressed in human medulloblastomas. Nature 428: 337-341.

29. Armstrong L, Hughes O, Yung S, Hyslop L, Stewart R, Wappler I, Peters H, Walter T, et al. (2006) The role of PI3K/AKT, MAPK/ERK and NFkappabeta signalling in the maintenance of human embryonic stem cell pluripotency and viability highlighted by transcriptional profiling and functional analysis. Hum Mol Genet 15: 1894-1913.

30. Cavalli F, Remke M, Rampasek L, Peacock J, Shih D, Luu B, Garzia L. Torchia J, et al. (2017) Intertumoral Heterogeneity within Medulloblastoma Subgroups. Cancer cell 31(6): 737-754.e6

31. R Core Team (2018). R: A language and environment for statistical computing. R Foundation for Statistical Computing, Vienna, Austria. URL <https://www.R-project.org/>.

32. Ulgen E, Ozisik O, Sezerman OU. (2018) pathfindR: An R Package for Pathway Enrichment Analysis Utilizing Active Subnetworks. bioRxiv. DOI: <https://doi.org/10.1101/272450>.

33. Zanini C, Ercole E, Mandili G, Salaroli R, Poli A, Renna C, Papa V, Cenacchi G, et al. (2013) Medullospheres from DAOY, UW228 and ONS-76 cells: increased stem cell population and proteomic modifications. PLoS One 8: e63748.

34. Robinson G, Parker M, Kranenburg TA, Lu C, Chen X, Ding L, Phoenix TN, Hedlund E, et al. (2012) Novel mutations target distinct subgroups of medulloblastoma. Nature 488: 43-48.

35. Huether R, Dong L, Chen X, Wu G, Parker M, Wei L, Ma J, Edmonson MN, et al. (2014) The landscape of somatic mutations in epigenetic regulators across 1,000 paediatric cancer genomes. Nat Commun 5: 3630.

36. Hadjimichael C, Chanoumidou K, Papadopoulou N, Arampatzi P, Papamatheakis J, Kretsovali A (2015) Common stemness regulators of embryonic and cancer stem cells. World J Stem Cells 7: 1150-1184.

37. Liu N, Li S, Wu N, Cho KS (2017) Acetylation and deacetylation in cancer stem-like cells. Oncotarget 8: 89315-89325.

38. Schonberg DL, Lubelski D, Miller TE, Rich JN (2014) Brain tumor stem cells: Molecular characteristics and their impact on therapy. Mol Aspects Med 39: 82-101.

39. Manoranjan B, Wang X, Hallett RM, Venugopal C, Mack SC, McFarlane N, Nolte SM, Scheinemann K, et al. (2013) FoxG1 interacts with Bmi1 to regulate self-renewal and tumorigenicity of medulloblastoma stem cells. Stem Cells 31: 1266-1277.

40. Raso A, Mascelli S, Biassoni R, Nozza P, Kool M, Pistorio A, Ugolotti E, Milanaccio C, et al. (2011) High levels of PROM1 (CD133) transcript are a potential predictor of poor prognosis in medulloblastoma. Neuro Oncol 13: 500-508.

41. Chen KH, Hsu CC, Song WS, Huang CS, Tsai CC, Kuo CD, Hsu HS, Tsai TH, et al. (2010) Celecoxib enhances radiosensitivity in medulloblastoma-derived CD133-positive cells. Childs Nerv Syst 26: 1605-1612.

42. Chang CJ, Chiang CH, Song WS, Tsai SK, Woung LC, Chang CH, Jeng SY, Tsai CY, et al. (2012) Inhibition of phosphorylated STAT3 by cucurbitacin I enhances chemoradiosensitivity in medulloblastoma-derived cancer stem cells. Childs Nerv Syst 28: 363-373.

43. Zakrzewska M, Zakrzewski K, Gresner SM, Piaskowski S, Zalewska-Szewczyk B, Liberski PP (2011) Polycomb genes expression as a predictor of poor clinical outcome in children with medulloblastoma. Childs Nerv Syst 27: 79-86.

44. Wang X, Venugopal C, Manoranjan B, McFarlane N, O'Farrell E, Nolte S, Gunnarsson T, Hollenberg R, et al. (2012) Sonic hedgehog regulates Bmi1 in human medulloblastoma brain tumor-initiating cells. Oncogene 31: 187-199.

45. MacDonald TJ, Brown KM, LaFleur B, Peterson K, Lawlor C, Chen Y, Packer RJ, Cogen P, et al. (2001) Expression profiling of medulloblastoma: PDGFRA and the RAS/MAPK pathway as therapeutic targets for metastatic disease. Nat Genet 29: 143-152.

46. Tabu K, Kimura T, Sasai K, Wang L, Bizen N, Nishihara, H. Taga T, Tanaka S, et al. (2010) Analysis of an alternative human CD133 promoter reveals the implication of Ras/ERK pathway in tumor stem-like hallmarks. Mol Cancer 9: 39.

47. Ozaki K, Minoda A, Kishikawa F, Kohno M (2006) Blockade of the ERK pathway markedly sensitizes tumor cells to HDAC inhibitor-induced cell death. Biochem Biophys Res Commun 339: 1171-1177.

48. Ozaki K, Kosugi M, Baba N, Fujio K, Sakamoto T, Nishihara H, Taga T, Tanaka S (2010) Blockade of the ERK or PI3K-Akt signaling pathway enhances the cytotoxicity of histone deacetylase inhibitors in tumor cells resistant to gefitinib or imatinib. Biochem Biophys Res Commun 391: 1610-1615.

49. Ishiguro T, Ohata H, Sato A, Yamawaki K, Enomoto T, Okamoto K (2017) Tumor-derived spheroids: Relevance to cancer stem cells and clinical applications. Cancer Sci 108: 283-289.

50. Ciccarelli C, Vulcano F, Milazzo L, Gravina GL, Marampon F, Macioce G, Giampaolo A, Tombolini, V (2016) Key role of MEK/ERK pathway in sustaining tumorigenicity and in vitro

radioresistance of embryonal rhabdomyosarcoma stem-like cell population. Mol Cancer 15: 16.

51. Sunayama J, Matsuda K, Sato A, Tachibana K, Suzuki K, Narita Y, Shibui S, Sakurada K, et al. (2010) Crosstalk between the PI3K/mTOR and MEK/ERK pathways involved in the maintenance of self-renewal and tumorigenicity of glioblastoma stem-like cells. Stem Cells 28: 1930-1939.

52. Adamson PC, Houghton PJ, Perilongo G, Pritchard-Jones K (2014) Drug discovery in paediatric oncology: roadblocks to progress. Nat Rev Clin Oncol 11: 732-739.

Table 1. Forward and reverse primers used for RT-qPCR amplification

Gene	Primer sense	Primer anti-sense
ACTB	5'- AAA CTG GAA CGG TGA AGG TG -3'	5'- AGA GAA GTG GGG TGG CTT TT -3'
BMI1	5´- TGC TTT GTG GAG GGT ACT TC -3'	5'- GTC TGG TCT TGT GAA CTT GGA -3'
CD133	5' GGC AAA TCA CCA GGT AAG AAC-3'	5'- AAC GCC TTG TCC TTG GTA G-3´

Legends for figures

Fig. 1. HDAC inhibition hinders the viability of MB cells. **a** Daoy and D283 cells were treated with different concentrations of NaB, and the number of living cells was quantified using trypan blue exclusion assays. **b** H3 acetylation was determined by ELISA. Results represent the mean ± SD. of three independent experiments. ** $P < 0.01$; **** $P < 0.0001$ compared to controls (Ctr).

Fig. 2. HDAC inhibition reduces stemness in MB cells. **a** Representative boxplot of *CD133* and *BMI1* expression in the medulloblastoma molecular subgroups from Cavalli *et al.* **b** Relative mRNA levels of stemness markers were determined in control and NaB-treated Daoy and D283 MB cells by RT-qPCR using primers specific for *BMI1* and *CD133* as described in Materials and Methods. **c** Daoy and D283 cells were treated with different concentrations of NaB for 24 or 48h, cells were then harvested and the expression of BMI1 and β-actin (loading control) was determined by Western blot analysis. The relative expression of BMI1 (24 or 48 h), were determined by densitometric analysis of signals normalized for the corresponding β-actin signal. The analysis was performed using Image J software (NIH, Bethesda, MD). Results represent the mean ± SD of three independent experiments; * $P < 0.05$; ** $P < 0.01$; *** $P < 0.001$; **** $P < 0.0001$ compared to controls (Ctr).

Fig. 3. HDAC inhibition reduces ERK activation in MB cells. **a** Balloon plot of the 10 most representative KEGG pathways of *CD133* or *BMI1* correlated genes. # of CGs: number of correlated genes. Large circles indicate higher number of correlated genes. A darker color indicates

a more significant *P* value **b** Daoy and D283 cells were treated with different concentrations of NaB for 24 or 48 h, cells were then harvested and the expression ERK, pERK and β-actin (loading control) was determined by Western blot analysis. The relative expression of ERK and p-ERK (48 h) were determined by densitometric analysis of signals normalized for the corresponding β-actin signal. The analysis was performed using Image J software (NIH, Bethesda, MD). Results represent the mean ± SD of three independent experiments; * $P < 0.05$; ** $P < 0.01$; *** $P < 0.001$; **** $P < 0.0001$ compared to controls (Ctr).

Fig. 4. Inhibition of HDAC and ERK impairs MB cell proliferation. **a** Relative mRNA levels of stemness markers were determined in control and U0126 -treated Daoy and D283 MB cells by RT-qPCR, using primers specific for *BMI1* and *CD133*. **b** Daoy and D283 cells were treated with different concentrations of NaB alone or in combination with the ERK inhibitor U0126, and the number of living cells were quantified using trypan blue exclusion assays. Results represent the mean ± SD of three independent experiments; * $P < 0.5$; ** $P < 0.01$; *** $P < 0.001$; **** $P < 0.0001$ compared to controls (Ctr); $^{\#} P < 0.05$; $^{\#\#} P < 0.01$; $^{\#\#\#} P < 0.001$; $^{\#\#\#\#} P < 0.0001$ compared to respective NaB dose; $^{\&} P < 0.05$; $^{\&\&\&\&} P < 0.0001$ compared to respective U0126 dose.

Fig. 5. ERK inhibition avoid MB stem cell formation. **a** Daoy and D283 cells were cultured in medium specific for stem cell expansion during 7 days for enrichment of neurospheres. Relative mRNA levels of stemness markers were determined in monolayer (M) and sphere (S) cultures by RT-qPCR using primers specific for *BMI1* and *CD133* as described in Materials and Methods. **b** Representative photomicrographs of neurospheres after 7 days of induction in the absence (Ctr) or

presence of the ERK inhibitor U0126 (12.5 or 25 μM) in the first day of induction. Results represent the mean ± SD of three independent experiments; ** $P < 0.01$; *** $P < 0.001$; **** $P < 0.0001$ compared to controls.

Figure 1

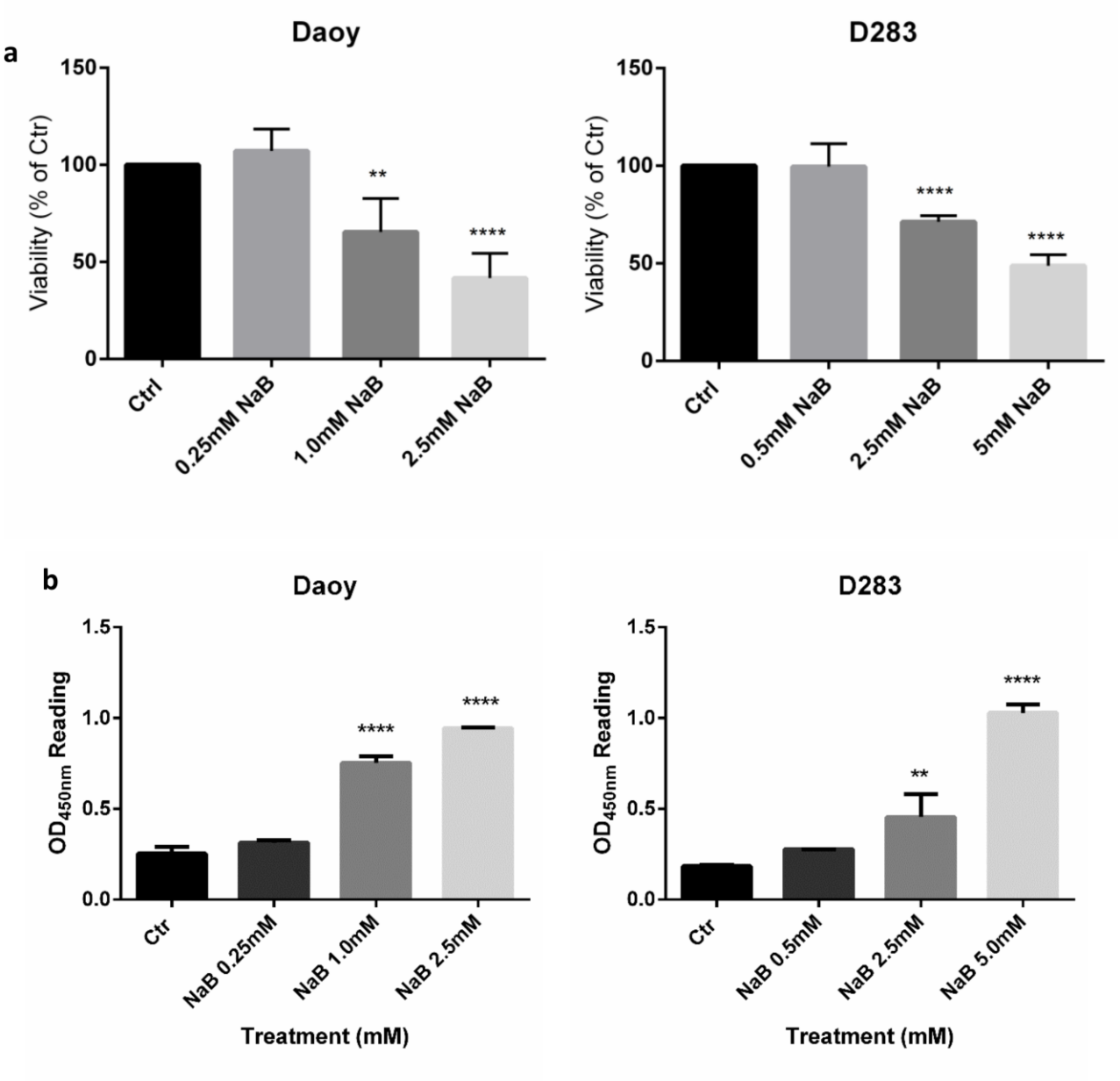

Figure 2

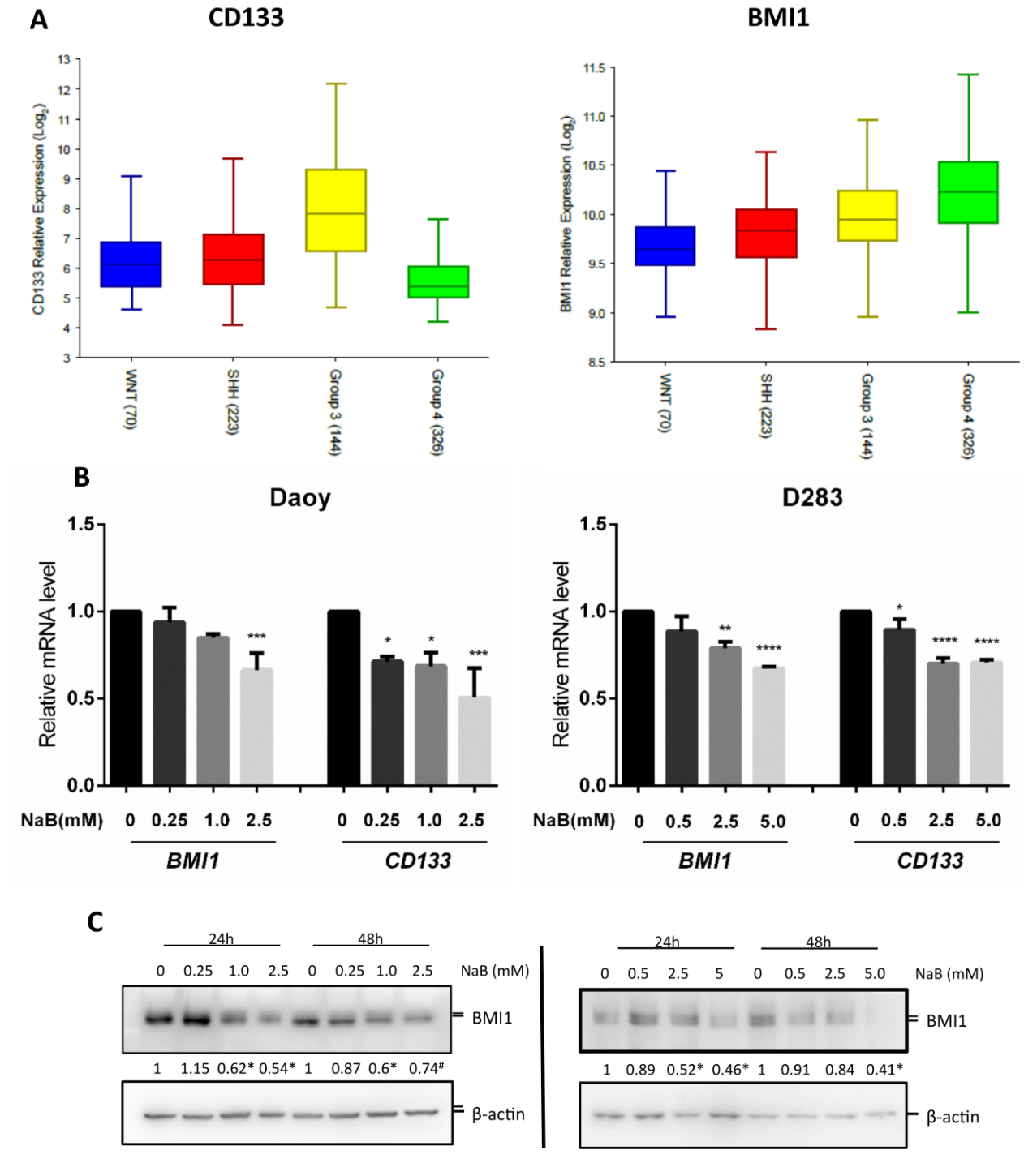

Figure 3

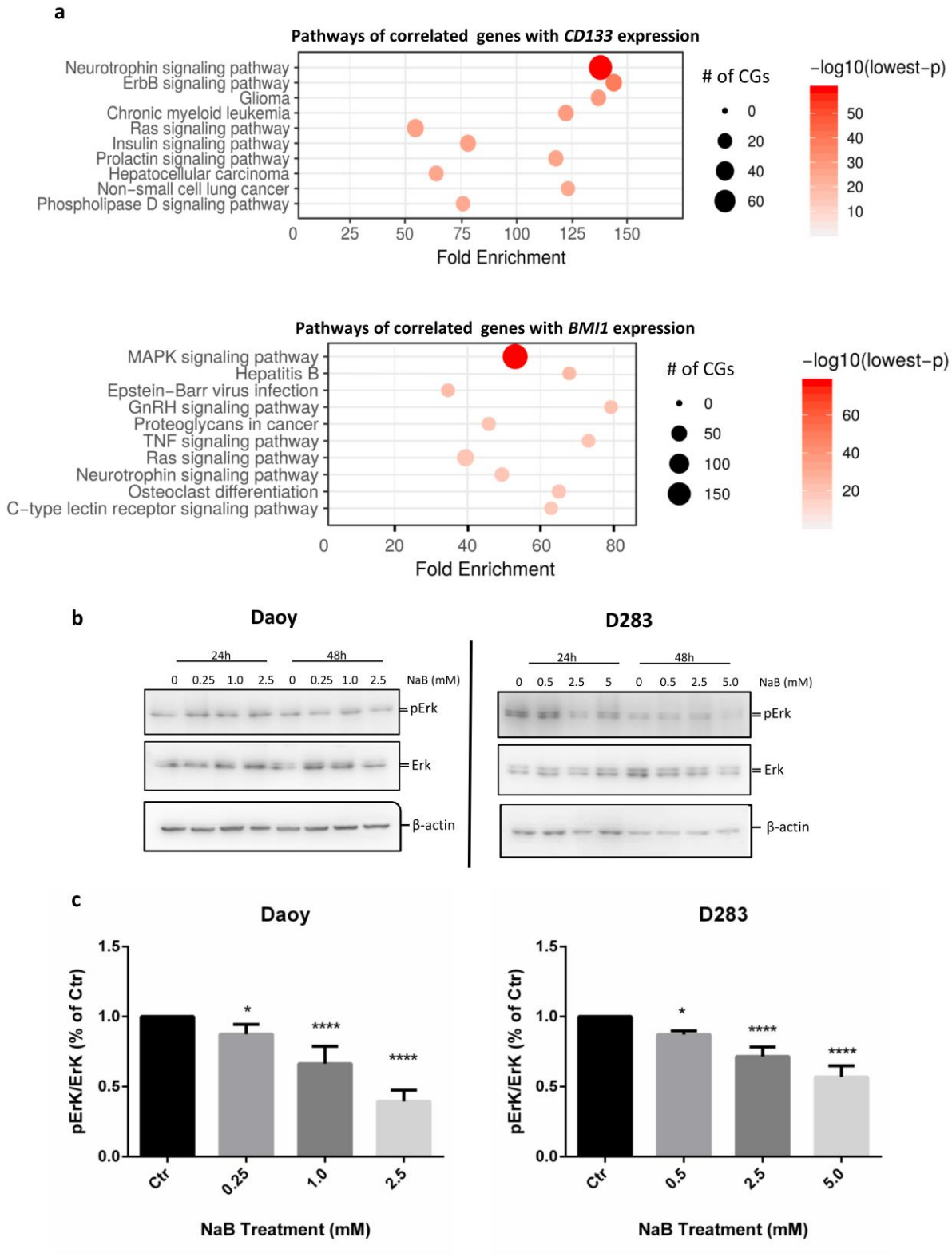

Figure 4

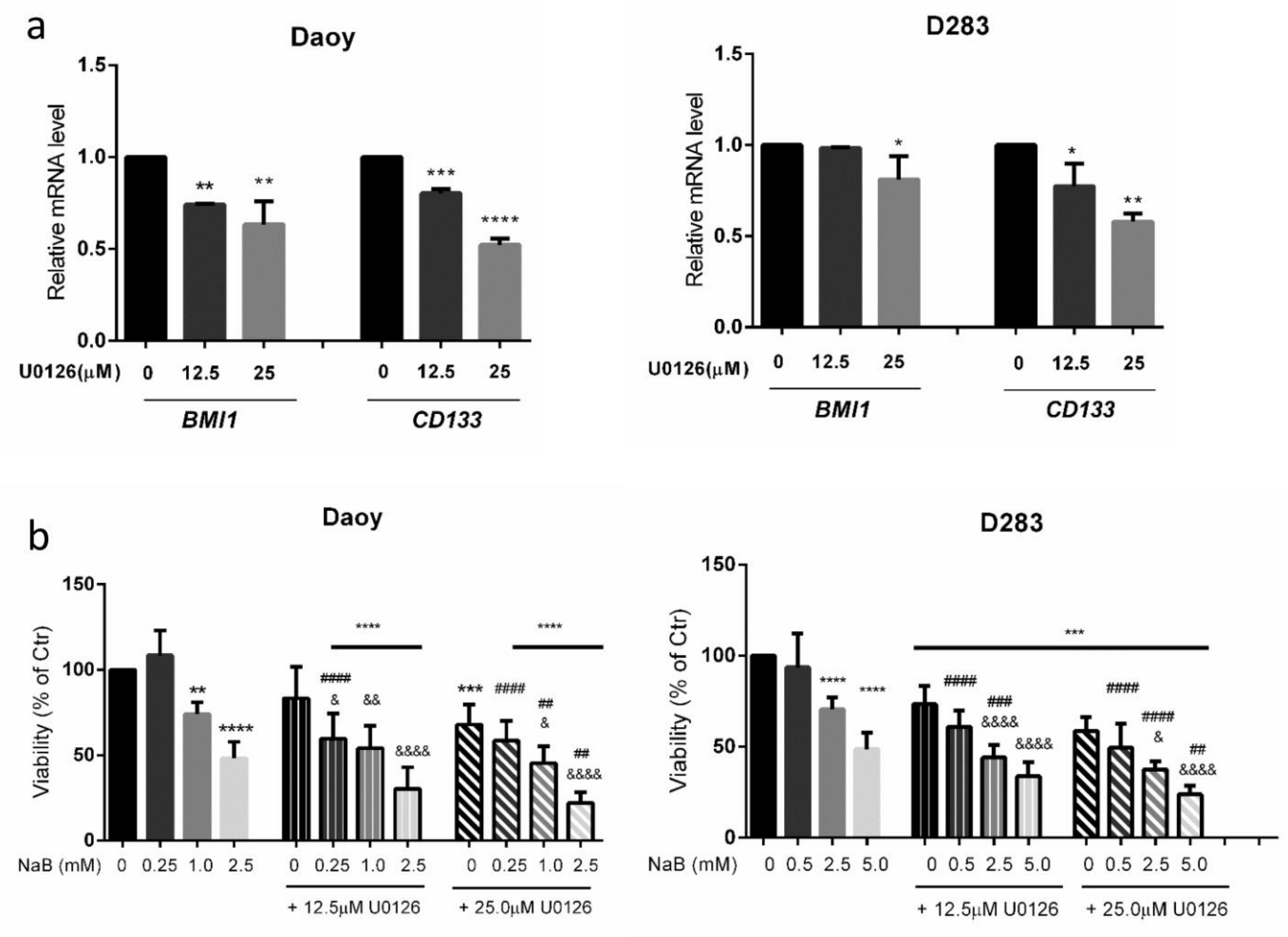

Figure 5